nature catalysis

ARTICLES

https://doi.org/10.1038/s41929-019-0357-9

Photocatalytic regio- and stereoselective C(sp^3)–H functionalization of benzylic and allylic hydrocarbons as well as unactivated alkanes

Yanjun Li, Meng Lei and Lei Gong*

The selective functionalization of inert C(sp^3)–H bonds is extremely attractive in organic synthesis and catalysis science, but the conversion of hydrocarbons lacking directing groups into chiral molecules through catalytic C(sp^3)–H functionalization is formidably challenging. Here, to address this problem, we have developed a photochemical system consisting of a hydrogen atom transfer organophotocatalyst and a chiral catalyst containing an earth-abundant metal. With the cooperative catalysts and imine partners, a wide range of benzylic, allylic hydrocarbons and unactivated alkanes can be converted to functionalized chiral products. The readily tunable bisoxazoline catalysts of copper or other metals exhibit precise regional recognition and asymmetric induction towards these inert C–H bonds. The reactions are applicable to many compounds including small hydrocarbons, branched alkanes, cycloalkanes and more complex medicinal agents. This method provides an economic and rapid construction of optically active compounds, starting from the most basic chemical feedstocks.

Conversions of the raw materials derived from petroleum or natural gas to value-added organic compounds is of great interest and importance in both academia and industry[1]. The direct C(sp^3)–H functionalization of pure hydrocarbons such as unactivated alkanes is extremely attractive[2–13]. Such transformations could have a broad potential in organic synthesis due to their step and atom economy and the abundance of starting materials[14]. The intrinsic chemical inertness of the C(sp^3)–H bonds, however, presents a big obstacle to such methods achieving useful reactivity and selectivity. The strategies of directing groups[15–18] and intramolecular hydrogen atom transfer (HAT) reactions[19,20] with the assistance of heteroatoms in the substrates have been successfully used to activate inert C(sp^3)–H bonds in a catalytic manner. Hydrocarbons with little or no difference in bond dissociation energies (BDEs) and polarity among their constituent atoms would appear to be outside the scope of these reactions. Recently, Davies and colleagues reported a highly sophisticated method that takes advantage of rhodium-carbene-induced C–H insertion to functionalize unactivated alkanes. The chiral dirhodium catalysts are key to both site recognition and asymmetric induction[21–24]. Despite these impressive advances, there remains a high demand for the development of economic and facile approaches to conversion of these most basic chemical feedstocks into valuable chiral molecules[25–27].

Visible-light photoredox catalysis has emerged as a powerful tool for the discovery of unique transformations[28–30], and the combination of photoredox and transition-metal catalysis provides a promising strategy for C–H functionalization[31–33]. For example, MacMillan et al. developed an effective synergistic catalytic system consisting of a decatungstate-anion-based photocatalyst and a nickel bipyridine complex for the C(sp^3)–H alkylation of cycloalkanes[31]. The groups of Molander[32] and Doyle[33] independently demonstrated that the merger of an iridium-based photocatalyst and a nickel catalyst could efficiently catalyse the direct cross-coupling of aryl bromides with α-hetero substituted/benzylic C(sp^3)–H bonds or chloroformates with cycloalkanes. Since these photochemical processes involve extremely active alkyl radical intermediates, it is inherently difficult to control their regio- and stereoselectivity. Consequently, the direct conversion of unactivated alkanes into functionalized chiral molecules through a radical pathway remains an unsolved problem. We posit that the following requirements should be satisfied to achieve this aim: (1) the reaction partners should be well matched in reactivity with the generated alkyl radicals to effectively reduce side reactions such as self-couplings; (2) the chiral catalyst must be able to recognize the background and catalysed radical transformations, thus encouraging asymmetric induction; (3) the catalyst control is better employed in the determination of which site in the substrate will be functionalized, thereby improving regioselectivity; and (4) the catalysts should be inexpensive and readily available for the development of economical methods.

This paper describes our efforts towards this goal. By employing cooperative catalysts consisting of a commercially available HAT organophotocatalyst (5,7,12,14-pentacenetetrone), a readily tunable chiral catalyst of earth-abundant metal (BOX-M, where M represents Cu or Co, and BOX represents chiral bisoxazoline) and *N*-sulfonylimines as the reaction partners, the highly selective C(sp^3)–H functionalization of benzylic, allylic hydrocarbons and unactivated alkanes has been achieved with visible light under mild conditions. The BOX catalysts of copper or cobalt exhibit precise regional and chiral recognition of the native C(sp^3)–H bonds. The reactions proceed with good to excellent yields, high regio- and stereoselectivity (up to >50:1 r.r. and 99.5% e.e.) (Fig. 1).

Results

Initial design and mechanistic hypothesis. Aryl ketones and quinones have been recently reported as one class of useful HAT photocatalysts, which exhibit potential in the catalytic activation of inert C–H bonds[34–37]. We selected 5,7,12,14-pentacenetetrone (**PT**)[38], a commercially available conjugate quinone, as the visible-light HAT photocatalyst with which to initiate the alkyl radical formation. BOX complexes of non-precious metals, which we recently showed[39,40]

Key Laboratory of Chemical Biology of Fujian Province, iChEM, College of Chemistry and Chemical Engineering, Xiamen University, Xiamen, Fujian, China.
*e-mail: gongl@xmu.edu.cn

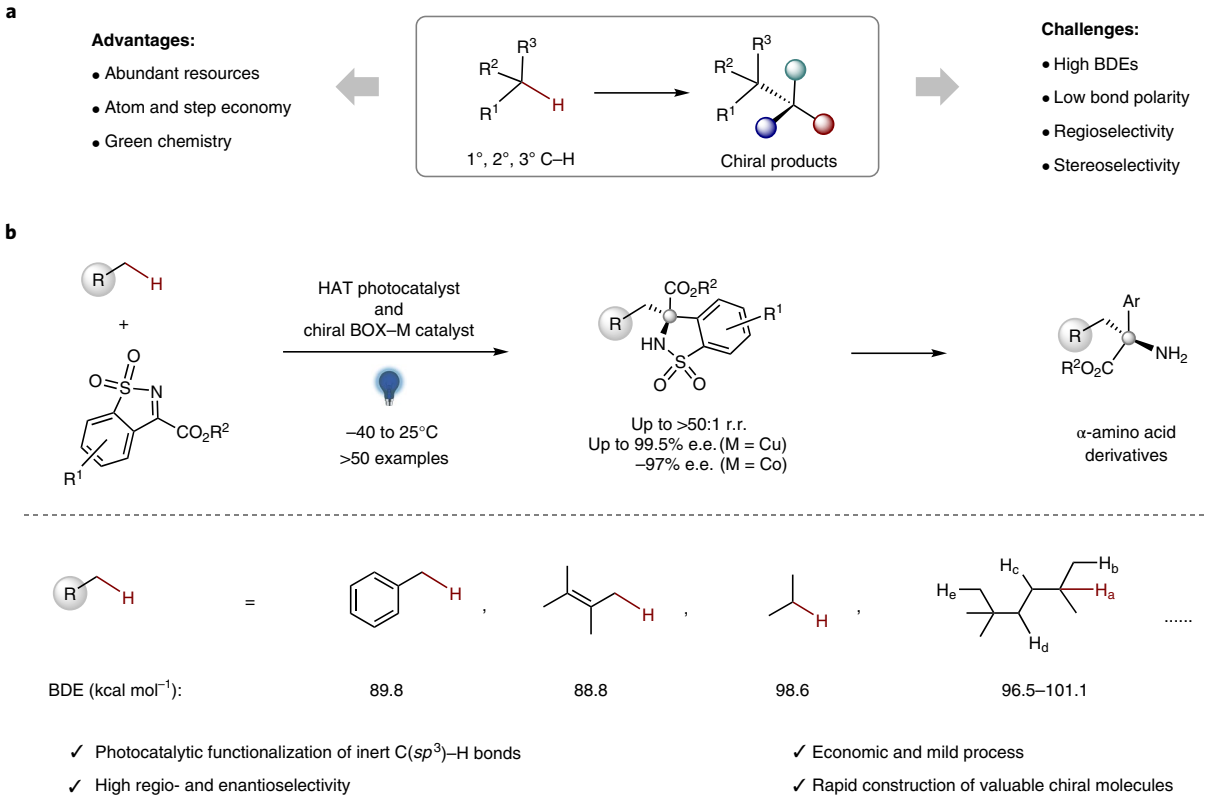

Fig. 1 | Direct and selective C(sp^3)–H functionalization of pure hydrocarbons. a, The advantages and challenges of selective C(sp^3)–H functionalization of pure hydrocarbons. **b**, The current study describes a photocatalytic system consisting of a HAT organophotocatalyst and a chiral catalyst of earth-abundant metal to provide a straightforward solution for regio- and stereoselective C(sp^3)–H functionalization of inert hydrocarbons: from benzylic, allylic hydrocarbons to unactivated alkanes, r.r. = regiomeric ratio, e.e. = enantiomeric excess.

to be highly efficient for asymmetric induction in photochemical transformations, were considered as the chiral catalysts. α-Carbonyl imines were chosen as the reaction partners, providing a means to convert the simple hydrocarbons to highly valuable chiral α-amino acids derivatives[41]. Notably, in the imine structures, the *N*-protecting group (R^1) and ester moiety were introduced to tune their reactivity as well as to fix the configuration and enable sufficient transition-metal activation through bidentate chelation. It is assumed that the chiral metal catalyst plays a key role in activation of the imine substrates to match with the generated alkyl radicals, which is an example of both sterically driven site recognition and asymmetric induction (Fig. 2a).

A proposed mechanism for the selective C(sp^3)–H functionalization of unactivated hydrocarbons is shown in Fig. 2b. The photocatalyst **PT** is excited by visible light to afford a long-lived triplet state, the biradical species **I** (τ[Ph_2CO] = 6.5 μs)[34], which then undergoes hydrogen atom abstraction from the inert C(sp^3)–H bond to generate the semiquinone-type radical (**II**) and alkyl radical (**III**)[38]. We speculated that both the steric hindrance on the HAT photocatalyst and the inherent stability of generated alkyl radicals would lead to a significant rate difference of C–H bond activation (Fig. 2a)[42]. Meanwhile, the imine substrate coordinates with the chiral metal catalyst, giving intermediate **IV**, and this is followed by a single electron transfer (SET) with **II** to close the photocatalytic cycle, concurrently affording the metal-stabilized carbon radical (**V**)[43]. The cross-coupling of the transient radical (**III**) and the persistent radical (**V**) generates an intermediate complex (**VI**), in which the regio- and stereoselectivity are sterically governed by the chiral ligand–transition-metal moiety. At this stage, the reactivities of the hydrocarbon and imine substrates are required to be well matched to precede the self-coupling of α-aminoalkyl radicals or alkyl radicals. A final protonation and ligand substitution lead to the formation of the product and regeneration of the coordinated imine (**IV**).

Reaction development. To explore the possibility of using the aforementioned co-catalyst system for the selective functionalization of C(sp^3)–H bonds, we selected toluene, which has a relatively lower bond dissociation energy (BDE = 89.8 kcal mol^{-1})[44], as the initial model substrate, α-carbonyl imines (**1a–1d**) as the reaction partners, and **PT** and a BOX copper complex generated in situ as the catalysts. The mixture of toluene, imine (**1a** or **1b**), the photocatalyst (**PT**) and premixed copper salt $Cu(BF_4)_2 \bullet H_2O$ (10 mol%) and the chiral ligand (**L1**) (11 mol%) in chloroform was stirred at 25 °C under argon with irradiation from a 24 W blue light-emitting diode (LED) lamp (maximum wavelength λ_{max} = 455 nm). The desired products (**2a** and **2b**) were not obtained (Table 1, entries 1 and 2), but the reaction of **1c** bearing an oxathiazine moiety afforded product **2c** in a quantitative yield with 45% e.e. (entry 3). The reaction of ethyl benzo[*d*]isothiazole 1,1-dioxide (**1d**) provided a similar reaction rate and a better enantioselectivity of 63% (entry 4). These results demonstrate that a well-matched imine partner is essential for the transformation in terms of the reactivity and selectivity. In comparison, removing **PT** or replacing it with other metal-based photocatalysts (entries 5–7), stirring the mixture in the dark at room temperature (entry 8) or at 80 °C (entry 9) were all reactions that failed.

Ligand screening experiments revealed that the BOX ligand **L5** led to the best enantioselectivity (91% e.e., entries 10–15). A copper(I) salt, $Cu(MeCN)_4BF_4$, was also tested in this reaction and provided a similar reaction rate but a lower enantioselectivity of 80% e.e. (entry 16). The photocatalytic system was established to be compatible with water and methanol (entries 17 and 18), but sensitive

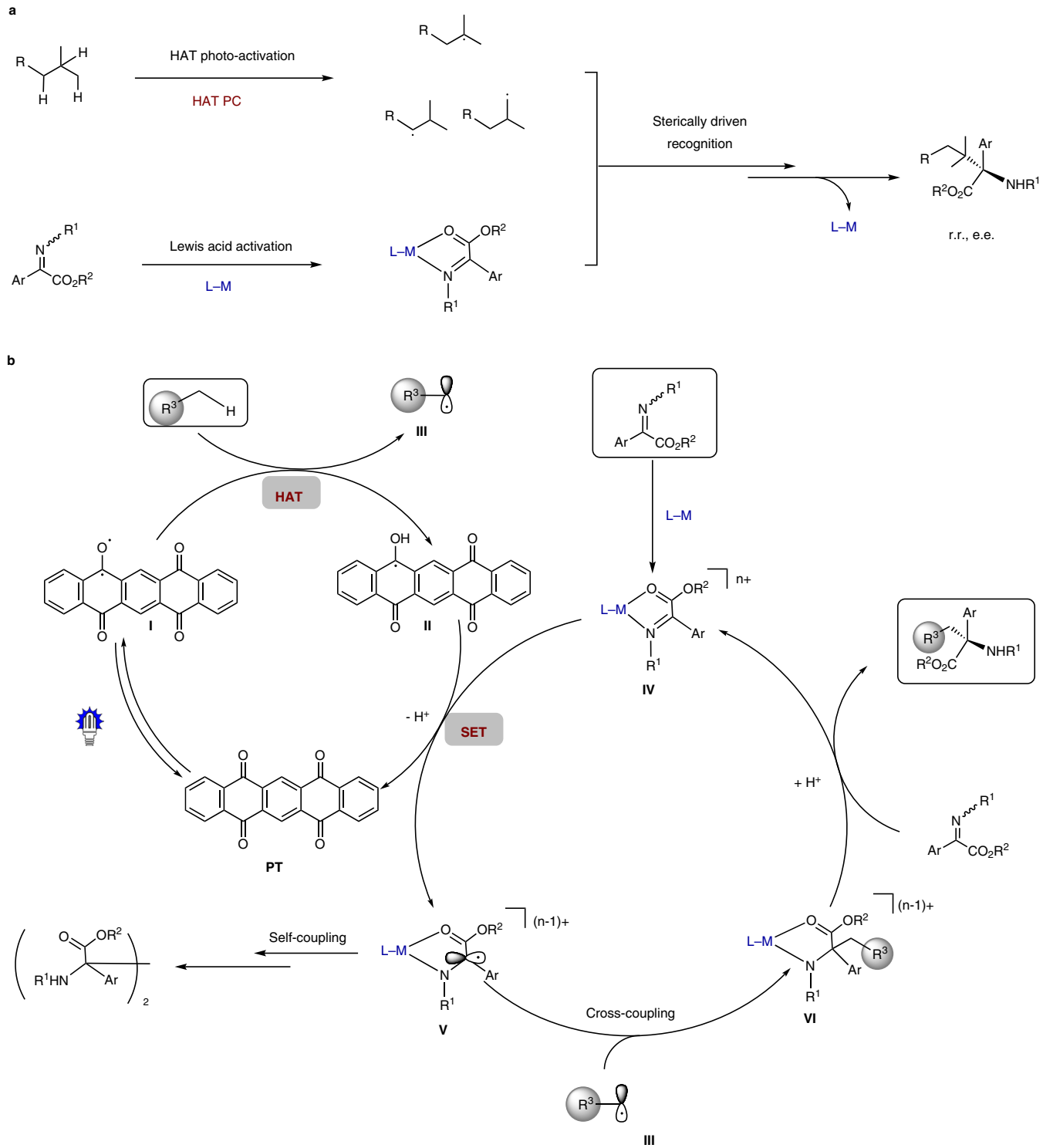

Fig. 2 | Initial design and mechanistic hypothesis. a, Our strategy involving a HAT organophotocatalyst and a chiral Lewis acid catalyst to functionalize C(sp^3)–H bonds of unactivated alkanes with regio- and stereoselectivity. PC, photocatalyst; L, chiral ligand. **b**, Mechanistic hypothesis.

to air (entry 19). Finally, we found that the enantioselectivity could be further improved to 93% e.e. by reducing the temperature to −20 °C (entry 20). It is worth noting that the reaction performed in a substrate ratio of 1:1 proceeded smoothly with a lower but reasonable reaction rate (86% conversion within 28 h) and the same enantioselectivity (entry 21). This result provides alternative conditions for functionalization of expensive substrates.

Reaction scope. We next evaluated the generality of the selective C(sp^3)–H functionalization with respect to pure hydrocarbons. First, a range of benzylic hydrocarbons (products **2d–16**) were tested (Fig. 3). The primary benzylic hydrocarbons (products **2d–8**) were well tolerated with regard to the yields (76–97%) and enantioselectivity (85–93% e.e.). The secondary benzylic hydrocarbons (products **9** and **10**) also exhibited good reactivity (88–95% yield) and

Table 1 | Optimization of reaction conditions

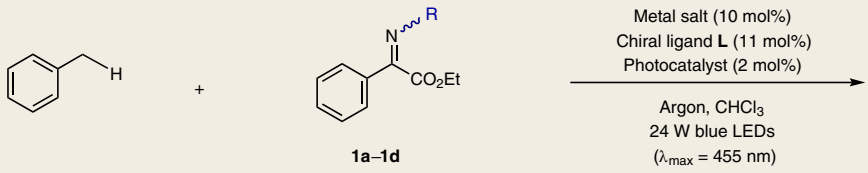

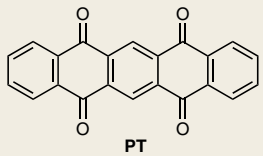
PT

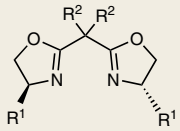
L1: R^1 = Ph, R^2 = Me
L2: R^1 = Ph, R^2 = Bn
L3: R^1 = *i*Pr, R^2 = Me
L4: R^1 = Ph, R^2 = CH_2Ph(4-*t*Bu)

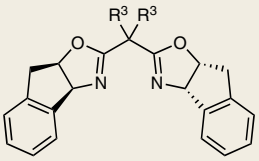
L5: R^3 = Me
L6: R^3 = CH_2Ph(4-*t*Bu)

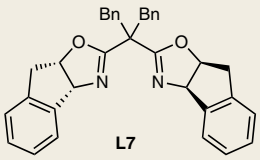
L7

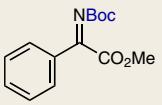
1a
E_{red} = –1.32 V
irreversible

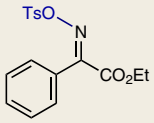
1b
E_{red} = –1.41 V
irreversible

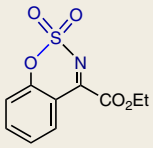
1c
$E_{1/2}$ = –0.58 V
reversible

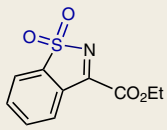
1d
$E_{1/2}$ = –0.49 V
reversible

Entry[a]	Metal salt	Ligand	Photocatalyst	Imine	*T* (°C)	*t* (h)	Conversion (%)[b]	e.e. (%)[c]
1	$Cu(BF_4)_2•H_2O$	**L1**	**PT**	**1a**	25	10	0	n.a.
2	$Cu(BF_4)_2•H_2O$	**L1**	**PT**	**1b**	25	10	0	n.a.
3[d]	$Cu(BF_4)_2•H_2O$	**L1**	**PT**	**1c**	25	10	Quant.	45
4	$Cu(BF_4)_2•H_2O$	**L1**	**PT**	**1d**	25	10	Quant.	63
5	$Cu(BF_4)_2•H_2O$	**L1**	None	**1d**	25	10	0	n.a.
6	$Cu(BF_4)_2•H_2O$	**L1**	$Ru(bpy)_3(PF_6)_2$	**1d**	25	10	0	n.a.
7	$Cu(BF_4)_2•H_2O$	**L1**	$Ir(ppy)_3$	**1d**	25	10	0	n.a.
8[e]	$Cu(BF_4)_2•H_2O$	**L1**	**PT**	**1d**	25	10	0	n.a.
9[e]	$Cu(BF_4)_2•H_2O$	**L1**	**PT**	**1d**	80	10	0	n.a.
10	$Cu(BF_4)_2•H_2O$	**L2**	**PT**	**1d**	25	10	Quant.	73
11	$Cu(BF_4)_2•H_2O$	**L3**	**PT**	**1d**	25	10	Quant.	48
12	$Cu(BF_4)_2•H_2O$	**L4**	**PT**	**1d**	25	10	Quant.	80
13	$Cu(BF_4)_2•H_2O$	**L5**	**PT**	**1d**	25	10	Quant.	91
14	$Cu(BF_4)_2•H_2O$	**L6**	**PT**	**1d**	25	10	Quant.	41
15	$Cu(BF_4)_2•H_2O$	**L7**	**PT**	**1d**	25	10	Quant.	–84
16	$Cu(MeCN)_4BF_4$	**L5**	**PT**	**1d**	25	10	Quant.	80
17[f]	$Cu(BF_4)_2•H_2O$	**L1**	**PT**	**1d**	25	10	Quant.	59
18[g]	$Cu(BF_4)_2•H_2O$	**L1**	**PT**	**1d**	25	10	Quant.	63
19[h]	$Cu(BF_4)_2•H_2O$	**L1**	**PT**	**1d**	25	10	0	n.a.
20	$Cu(BF_4)_2•H_2O$	**L5**	**PT**	**1d**	–20	24	Quant.	93
21[i]	$Cu(BF_4)_2•H_2O$	**L5**	**PT**	**1d**	–20	28	86	93

[a]Reaction conditions: toluene (1.0 mmol), **1a–1d** (0.10 mmol), metal salt (10 mol%), ligand (11 mol%), photocatalyst (2 mol%), $CHCl_3$ (2.0 ml), indicated temperature, 24 W blue LED lamp (λ_{max} = 455 nm), under argon; *T*, temperature; *t*, reaction time; Quant., quantitative yield. See more details in Supplementary Table 1 for the screening of solvent. [b]Conversion determined by ^{1}H-NMR. [c]e.e. value determined by chiral high-performance liquid chromatography. [d]The reaction of toluene and **1c** could be further improved by using $Co(acac)_2$ (10 mol%) as the salt and **L1** (11 mol%) as the chiral ligand, affording product **2c** in 95% yield and –93% e.e. (see more details in Supplementary Table 3). [e]Reaction performed in the dark. [f]Reaction performed in the presence of H_2O (10 equiv.). [g]Reaction performed in the presence of MeOH (10 equiv.). [h]Reaction performed in air. [i]Reaction performed in a substrate ratio of 1:1 (toluene: **1d**). n.a., not applicable.

enantioselectivity (90–98% e.e.), but no diastereoselectivity. The tertiary benzylic hydrocarbons (products **11**–**13**) performed favourably under the same reaction conditions to deliver the desired products with extremely high enantioselectivities (up to 99.5% e.e.). Notably, the functionalization of benzylic hydrocarbons displayed a certain degree of regioselectivity, which was not always consistent with the predicted stability of the corresponding carbon radicals (products **14**–**16**). For example, *p*-ethyl toluene (product

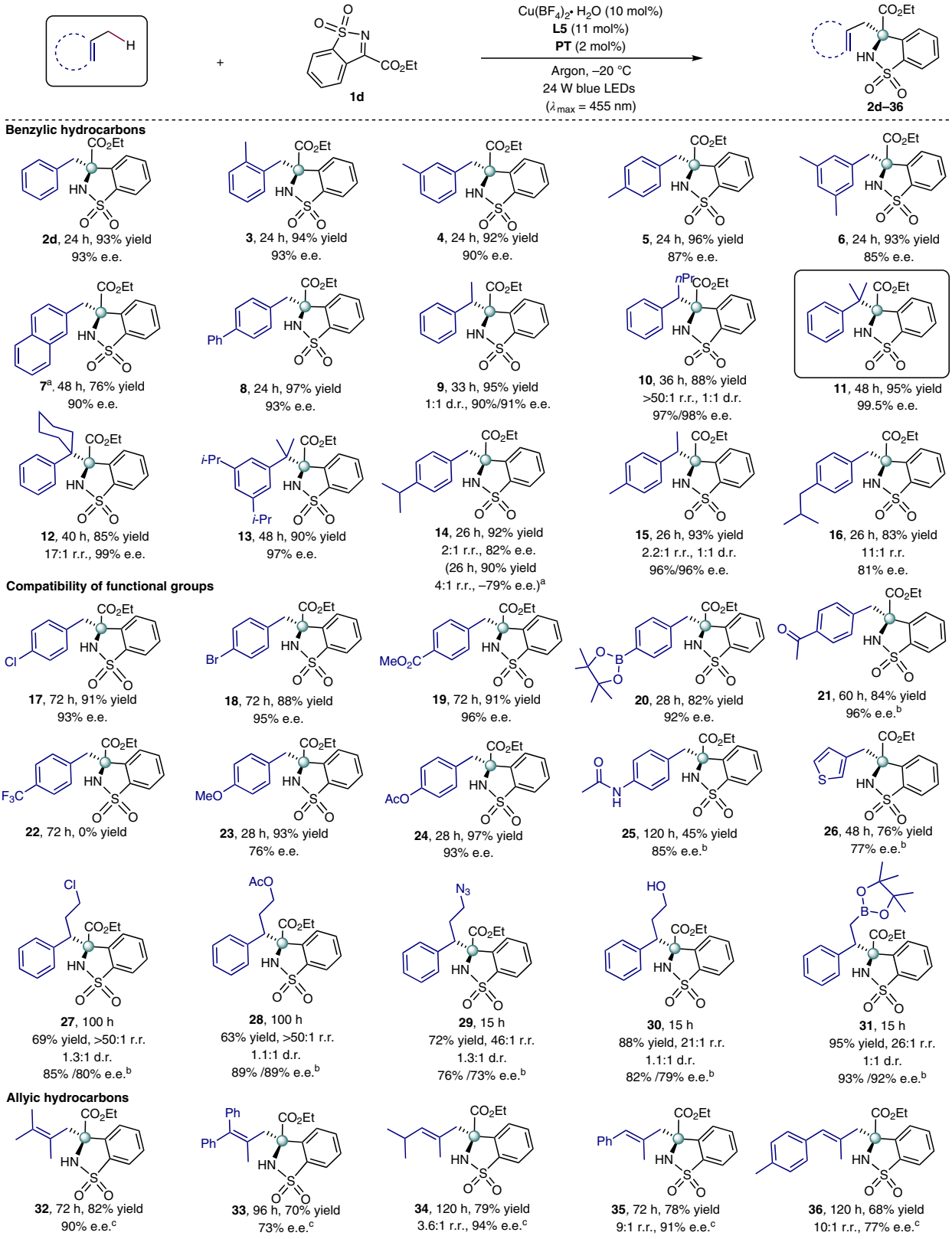

Fig. 3 | Reaction scope. Substrate scope of benzylic, allylic hydrocarbons and benzylic hydrocarbon derivatives. [a]Performed with **L7** as the chiral ligand. [b]Performed with $Cu(BF_4)_2 \cdot H_2O$ (10 mol%), **L5** (11 mol%), **PT** (2 mol%) at 25 °C. [c]Performed with $Cu(BF_4)_2 \cdot H_2O$ (20 mol%), **L5** (22 mol%), **PT** (5 mol%) at 25 °C. d.r., diastereomeric ratio.

15) preferred functionalization of secondary benzylic C–H bonds (r.r. = 2.2:1). In *p*-isopropyl toluene (product **14**) and *p*-isobutyl toluene (product **16**), the functionalization of primary benzylic C–H bonds was more favoured, providing 2:1–11:1 r.r.. In particular, the better regioselectivity (4:1) could be obtained by using a different bisoxazoline ligand **L7** for the reaction of *p*-isopropyl toluene. These

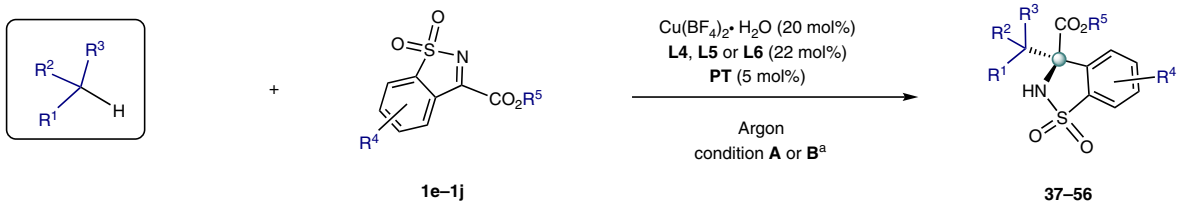

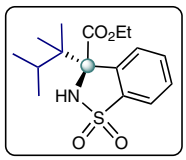

37, 26 h, 60% yield
>50:1 r.r., 97% e.e.
(condition **A**, **L5**)

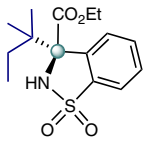

38, 48 h, 65% yield
9:1 r.r., 92% e.e.
(condition **B**, **L6**)

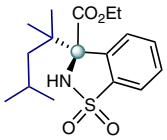

39, 30 h, 78% yield
>50:1 r.r., 88% e.e.
(condition **A**, **L5**)

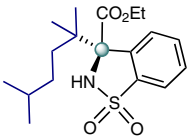

40, 72 h, 77% yield
>50:1 r.r., 84% e.e.
(condition **B**, **L5**)

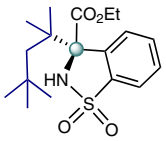

41, 40 h, 54% yield
>50:1 r.r., 96% e.e.
(condition **A**, **L5**)

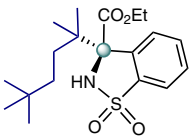

42, 57 h, 71% yield
>50:1 r.r., 73% e.e.
(condition **B**, **L5**)

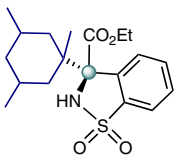

43, 48 h, 82% yield
>50:1 r.r., 71% e.e.
(condition **B**, **L5**)

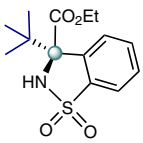

44[b], 48 h, 79% yield
>50:1 r.r., 69% e.e.
(condition **B**, **L6**)

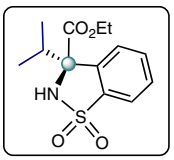

45[c], 48 h, 35% yield
>50:1 r.r., 39% e.e.
(condition **B**, **L4**)

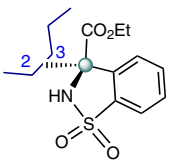

46, 28 h, 18% yield
2/3 = 2:1
d.r.(2) = 1:1
(condition **A**, **L4**)

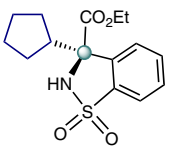

47, 10 h, 31% yield
36% e.e.
(condition **B**, **L4**)

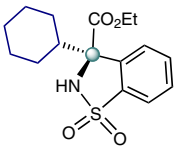

48, 10 h, 56% yield
5% e.e.
(condition **B**, **L4**)

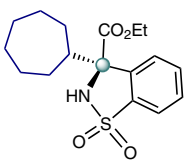

49, 10 h, 62% yield
60% e.e.
(condition **B**, **L4**)

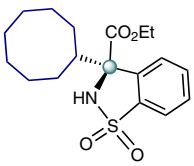

50, 10 h, 81% yield
69% e.e.
(condition **B**, **L4**)

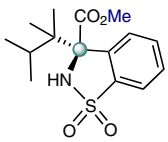

51, 26 h, 75% yield
>50:1 r.r., 97% e.e.
(condition **A**, **L5**)

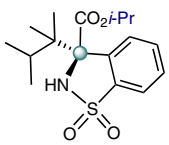

52, 26 h, 73% yield
>50:1 r.r., 98% e.e.
(condition **A**, **L5**)

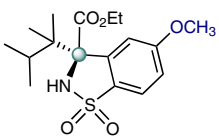

53, 26 h, 61% yield
>50:1 r.r., 96% e.e.
(condition **A**, **L5**)

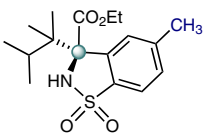

54, 26 h, 52% yield
>50:1 r.r., 97% e.e.
(condition **A**, **L5**)

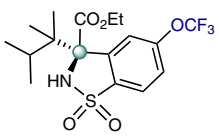

55, 20 h, 66% yield
>50:1 r.r., 94% e.e.
(condition **A**, **L5**)

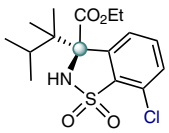

56, 20 h, 75% yield
>50:1 r.r., 96% e.e.
(condition **A**, **L5**)

Fig. 4 | Reaction scope. Substrate scope of unactivated secondary and tertiary alkanes and *N*-sulfonylimines. [a]Condition **A**: −40 °C, 50 W blue LEDs (λ_{max} = 420 nm). Condition **B**: 25 °C, 24 W blue LEDs (λ_{max} = 455 nm). [b]Reaction performed in the presence of isobutane (5 equiv.). [c]Reaction performed in the presence of propane (21 equiv.).

outcomes suggested that regioselectivity of the photochemical reactions is governed by the catalysts in addition to the inherent stability difference of generated carbon radicals[45,46].

The functional group compatibility of this reaction was also investigated (products **17**–**31**). The toluene-type substrates containing electron-withdrawing moieties, such as halogens, ester, boron ester or keto groups (products **17**–**21**), electron-donating groups (products **23**–**25**) on the phenyl ring or α-methyl heterocylic compound (product **26**), all exhibited excellent reactivity and enantioselectivity (76–96% e.e.). Moreover, a range of substituents on the alkyl chain were also tolerated. For example, the reaction of (3-chloropropyl)benzene (product **27**), 3-phenylpropyl acetate (product **28**), (3-azidopropyl)benzene (product **29**), 3-phenylpropan-1-ol (product **30**) or 4,4,5,5-tetramethyl-2-phenethyl- 1,3,2-dioxaborolane (product **31**) all provided the desired product in 63–95% yield, and with excellent regioselectivity

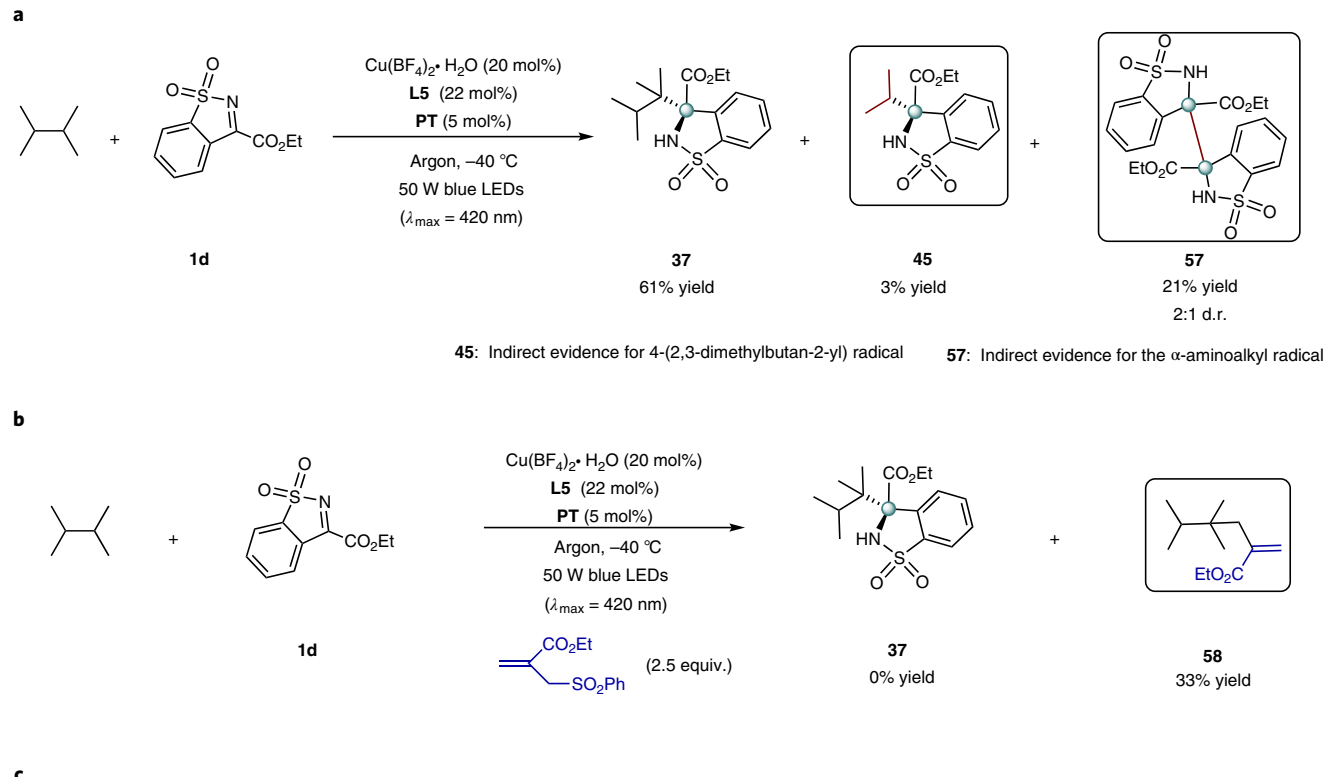

Entry[a]	Metal salt	*t* (h)	Conversion (%)[b]	e.e. (%)[c]	Entry	Metal salt	*t* (h)	Conversion (%)[b]	e.e. (%)[c]
1[d]	$Cu(BF_4)_2 \cdot H_2O$	10	Quant.	63	4	$Zn(BF_4)_2 \cdot H_2O$	10	68	–68
2	None	10	18	n.d.	5	$Co(BF_4)_2 \cdot 6H_2O$	10	Quant.	–87
3	$Ni(BF_4)_2 \cdot 6H_2O$	10	Quant.	–85	6	$Co(OAc)_2$	10	Quant.	–97

Fig. 5 | Mechanistic study. a, Isolation of the side products. **b**, Interference with a radical acceptor. **c**, Catalysis by chiral Lewis acids of other non-precious metals. [a]Reaction conditions: toluene (1.0 mmol), **1d** (0.10 mmol), metal salt (10 mol%), **L1** (11 mol%), **PT** (2 mol%), $CHCl_3$ (2.0 ml), 25 °C, 24 W blue LEDs, under argon. [b]Conversion determined by ^{1}H-NMR. [c]e.e. value determined by chiral high-performance liquid chromatography. [d]Taken from entry 4 of Table 1. n.d., not determined.

(up to 50:1 r.r.), low diastereoselectivity (1:1–1.3:1 d.r.) and high enantioselectivity (73–93% e.e.).

Allylic hydrocarbons (products **32**–**36**) were compatible with the system. The reaction of 2,3-dimethylbut-2-ene under the standard reaction conditions afforded the desired product **32** in 82% yield and with 90% e.e. The reaction rates of allylic hydrocarbons were lower than those of toluene derivatives, and a higher catalyst loading and reaction temperature were employed to promote these reactions. The reaction of 2,4-dimethylpent-2-ene provided a regioselectivity of 3.6:1 (the ratio of E/Z isomers of product **34**) in addition to an enantioselectivity of 94% e.e. Larger steric differences between the substituents on the C=C double bond led to a better regioselectivity (9:1 r.r., product **35**). The reaction of 1-methyl-4-(2-methylprop-1-en-1-yl) benzene exhibited a superior regioselectivity towards the allylic C–H bonds over benzylic C–H bonds (product **36**, 10:1 r.r., 77% e.e.).

With the results of benzylic and allylic substrate functionalization in hand, we questioned whether the photocatalytic system could be extended to more inert C(sp^3)–H precursors, such as unactivated alkanes with significantly higher bond dissociation energies (BDE = 96.5–104.9 kcal mol^{-1}) and more reactive radical intermediates[44]. This was indeed the case and we found that simple alkanes could react smoothly with the imines under the standard conditions with minor variations (Fig. 4). For example, one of the tertiary C–H bonds in 2,3-dimethylbutane was selectively functionalized, affording product **37** in 60% yield and 97% e.e. as a single regioisomer. Other branched-chain alkanes were examined, including 2-methylbutane (product **38**), 2,4-dimethylpentane (product **39**), 2,5-dimethylhexane (product **40**), 2,2,4-trimethylpentane (product **41**), 2,2,5-trimethylhexane (product **42**) and 1,3,5-trimethylcyclohexane (product **43**) (although the reaction of 1,3,5-trimethylcyclohexane showed an excellent site selectivity towards tertiary C–H bonds, the stereochemistry of product **43** was not clear; see ref. [24]), and they all exhibited a high level of regioselectivity (9:1–50:1 r.r.) and enantioselectivity (71–96% e.e). We speculate that the excellent

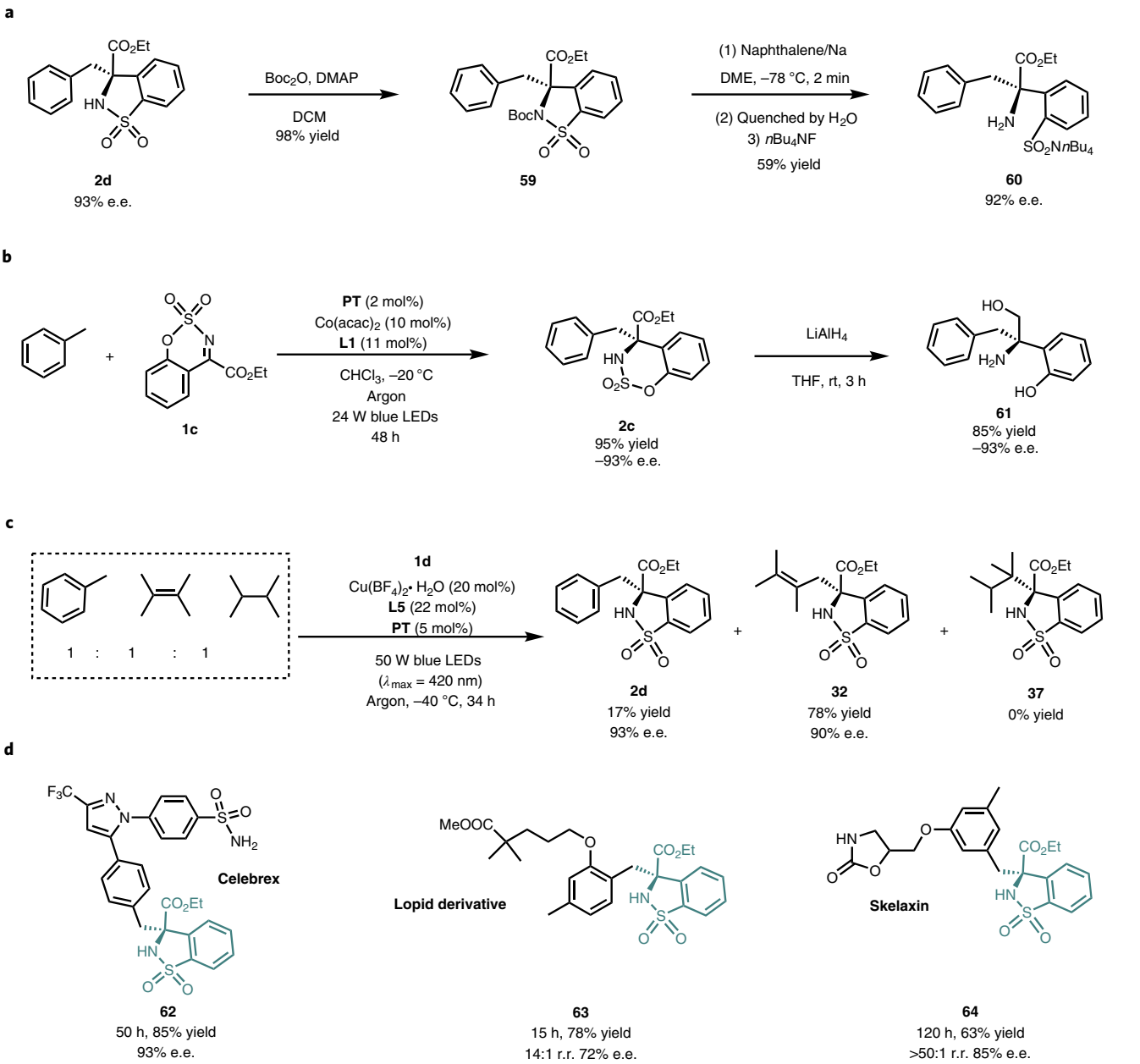

Fig. 6 | Synthetic utility of the method. a, Transformation of the product to an α-amino acid derivative. **b**, Synthetic application of this method into another imine. **c**, Selective functionalization of a hydrocarbon mixture. **d**, Late-stage diversification of medicinal agents under reaction conditions: $Cu(BF_4)_2•H_2O$ (20 mol%), **L5** (22 mol%), ratio of substrates = 1:1 (bioactive molecule, *N*-sulfonylimine), **PT** (5 mol%), 25 °C, 24 W blue LED. DMAP, dimethylaminopyridine; DCM, dichloromethane; DME, 1,2-dimethoxyethane; THF, tetrahydrofuran; rt, room temperature.

regioselectivity of compounds with tertiary C(sp^3)–H bonds could be attributed to not only the different formation rates of primary, secondary and tertiary carbon radicals, but also the steric recognition by the HAT photocatalyst and transition-metal catalyst (Fig. 2a)[42,44]. Furthermore, it was established that isobutane (product **44**) and propane (product **45**) were also tolerated in the reaction, which proceeded with higher reaction rates, exclusive regioselectivity and a reduced enantioselectivity of 69% e.e. and 39% e.e., respectively. These results demonstrate that the catalytic system delivers accurate regional and chiral recognition of very small alkane molecules.

This method was also applicable to functionalization of the secondary C–H bonds in cyloalkanes (products **47**–**50**). The reactions of cyclopentane, cyclohexane, cycloheptane or cyclooctane all delivered the desired product in 31–81% yield within 10 h (refs. [24,47]). Typically, larger cyclic alkanes were favoured regarding the yield and enantioselectivity, perhaps due to the appropriate conformation and steric hindrance.

Imine partners containing a distinct α-carbonyl group adjacent to the imino moiety (products **51** and **52**), and those with an electron-donating substituent (products **53** and **54**) or an electron-withdrawing substituent (products **55** and **56**) within the phenylsulfonyl ring were all compatible with the reaction. These reactions provided a range of optically active isothiazolidine 1,1-dioxides in 52–75% yield and with 94–98% e.e. as single regioisomers.

Mechanistic studies. The cyclic voltammetry of substrates **1a**–**1c** under argon was measured to estimate the redox ability of imines. As illustrated in Table 1 and Supplementary Figs. 4–6, the imine

substrates **1a** and **1b** show irreversible peaks at $E_{red} = -1.32$ V and −1.41 V, respectively. In contrast, the reactive substrates **1c** and **1d**[39] exhibit reversible reduction/oxidation peaks with much lower reduction potentials ($E_{1/2} = -0.58$ V and −0.49 V, respectively). Electrochemical studies suggest that the imine substrates with low reduction potentials and reversible redox activity, for example the reactive substrates **1c** and **1d**, might be required for completion of the photocatalytic cycle. These results are consistent with our mechanistic hypothesis of radical coupling of an α-aminoalkyl radical with an alkyl radical.

Several control experiments were conducted to examine the reaction pathway (Fig. 5). First, two unexpected side products **45** (3%) and **57** (21%) from the reaction 2,3-dimethylbutane + **1d**→**37** (Fig. 5a) were isolated. It was assumed that the unexpected product **45** was derived from addition of 2,3-dimethylbutan-2-yl radical to the imine substrate followed by 1,5-HAT, β-cleavage and SET process (see further details in Supplementary Method 5.6). This outcome provided indirect evidence of the alkyl radical formation in the photocatalytic C(sp^3)–H functionalization and also suggested that radical addition pathways could not be completely excluded (more details are available in Supplementary Fig. 8). Compound **57** was identified as a self-coupling product of the imine (**1d**), giving a strong indication of the reductive formation of the α-aminoalkyl radical. Interference of the photochemical reaction with a radical acceptor ethyl 2-((phenylsulfonyl)methyl)acrylate led to the formation of **58** (33%), further confirming the existence of an alkyl radical (Fig. 5b).

Functionalities of the metal catalysts in the photochemical transformation were also investigated (Fig. 5c)[48]. In the absence of a metal catalyst, the reaction toluene +**1d**→**2d** had a dramatically slower reaction rate (entry 2). Replacing the copper salt by the tetrafluoroborate salt of nickel, zinc or cobalt all led to efficient conversions, revealing that the transition-metal catalyst probably serves as a chiral Lewis acid (entries 3–6)[49]. The reactions catalysed by either zinc, nickel or cobalt, however, all afforded an inverted enantioselectivity compared to the reaction enabled by the copper complex with the same chiral ligand **L1** and under identical reaction conditions. For example, $Co(BF_4)_2{\bullet}6H_2O$ provided product **2d** quantitatively and with −87% e.e. within 10 h. Such a metal-induced configuration inversion of the products in the catalytic reaction has been reported only rarely. It is assumed that this result is determined by the coordination geometry of the different metals[50]. Moreover, a higher enantioselectivity of −97% was obtained when using a cobalt salt with coordinative anions, such as $Co(OAc)_2$. These results offer a potentially interesting opportunity to develop a stereodivergent synthesis by alternation of the metal centres.

The quantum yield (Φ) of the photochemical reaction was calculated to be 0.08, confirming that radical chain propagation was not the predominant mechanism (see further details in Supplementary Method 5.4).

Synthetic utility of the method. To establish the generality of this method, a straightforward transformation of the products was developed. As shown in Fig. 6a, compound **2d** was converted into the corresponding α-amino acid derivative (**60**) with 92% e.e. in a total yield of 58% by *N*-Boc protection followed by rapid treatment with naphthalene sodium and deprotection. Such disubstituted α-amino acid derivatives could serve as chiral building blocks for further elaboration[51].

This method is also applicable to other imines with well-matched reactivity and redox ability. For example, under the standard photocatalytic conditions and with **Co-L1** and **PT** as the cocatalysts, the reaction of ethyl benzo[*e*][1,2,3]oxathiazine-4-carboxylate 2,2-dioxide (**1c**) provided the desired product (**2c**) in 95% yield and with −93% e.e. **2c** could be readily coverted into the chiral amino alcohol (**61**) in 85% yield and with the retention of the absolute configuration by treatment with $LiAlH_4$ in THF (tetrahydrofuran) at room temperature for 3 h (Fig. 6b).

Moreover, if a 1:1:1 mixture of toluene, 2,3-dimethylbut-2-ene and 2,3-dimethylbutane was employed in the photochemical system, only the corresponding products **2d** and **32** were obtained in a ratio of 1:4.6 (Fig. 6c). The BDEs of toluene, 2,3-dimethylbut-2-ene and 2,3-dimethylbutane are 89.8, 88.8 and 98.6 kcal mol^{-1}, respectively. This observation is therefore consistent with the strength of these C(sp^3)–H bonds, and provides an approach to direct functionalization of hydrocarbon mixtures from petroleum or natural gas.

Finally, the method was applied to the late-stage diversification of drugs or other bioactive molecules. For example, the photocatalytic reaction of celebrex, a non-steroidal anti-inflammatory drug, delivered the functionalized product (**62**) in 85% yield and with 93% e.e. The reaction of a lopid derivative afforded **63** in 78% yield and with 14:1 r.r. and 72% e.e. within 10 h. Skelaxin, a muscle relaxant, could be converted to **64** in 63% yield and with >50:1 r.r. and 85% e.e. (Fig. 6d). In comparison to the rhodium-carbene-catalysed C–H functionalization, our method is less favoured in selective functionalizion of more complex molecules such as vitamin E and cholesterol acetate (see further details in Supplementary Method 3.4). Considering the importance of chiral medicinal agents, we expect that this methodology would be useful for chiral drug synthesis by the introduction of stereocentres at a very late stage.

Conclusion

We report the development of selective C(sp^3)–H functionalization of hydrocarbons by means of an efficient catalytic platform employing a synergistic combination of a HAT organophotocatalyst and a BOX catalyst of a non-precious transition metal. The native C(sp^3)–H bonds in a range of benzylic, allylic hydrocarbons and unactivated alkanes can be functionalized with good to excellent regioselectivity (up to >50:1 r.r.) and stereoselectivity (up to 99.5% e.e.). The method provides rapid and economic access to direct introduction of stereocentres to small molecules such as propane and isobutene, branched alkanes and more complicated medicinal agents such as celebrex and skelaxin. Further investigations on the mechanisms and applications of these reactions are in progress in the laboratory.

Methods

General. For the preparation of the 20 mM solution of copper catalyst **Cu^{ii}-L4**, **Cu^{ii}-L5**, **Cu^{ii}-L6** or **Cu^{ii}-L7** in $CHCl_3$, a solution of $Cu(BF_4)_2{\bullet}H_2O$ (25.5 mg, 0.100 mmol) and a BOX ligand **L4**, **L5**, **L6** or **L7** (0.110 mmol) in $CHCl_3$ (5.0 ml) was stirred at 40 °C for 1 h, and freshly prepared samples were used for the catalytic reactions.

General procedure for photocatalytic selective C(sp^3)–H functionalization of benzylic and allylic hydrocarbons. A dried 10 ml Schlenk tube was charged with **1d** (0.20 mmol), a benzylic or allylic hydrocarbon substrate (2.0 mmol), **PT** (1.40 mg, 0.0040 mmol, 2 mol%; or 3.40 mg, 0.010 mmol, 5 mol%), chiral copper catalyst **Cu^{ii}-L5** or **Cu^{ii}-L7** (1.0 or 2.0 ml taken from a 20 mM solution in $CHCl_3$) and $CHCl_3$ (3.0 or 2.0 ml). The mixture was degassed via three freeze–pump–thaw cycles. The Schlenk tube was positioned approximately 5 cm away from a 24 W blue LED lamp ($\lambda_{max} = 455$ nm). After being stirred at −20 °C or 25 °C for the indicated time, the reaction mixture was evaporated to dryness. The residue was purified by flash chromatography on silica gel and eluted with petroleum ether, EtOAc = 5:1, to afford the non-racemic product (**2d–36**).

General procedure for photocatalytic selective C(sp^3)–H functionalization of alkane substrates. A dried 25 ml Schlenk tube was charged with **1e–1j** (0.20 mmol), alkane substrates (2.0 mmol), **PT** (3.40 mg, 0.010 mmol, 5 mol%), chiral copper catalyst **Cu^{ii}-L4**, **Cu^{ii}-L5** or **Cu^{ii}-L6** (2.0 ml taken from the 20 mM solution in $CHCl_3$) and $CHCl_3$ (2.0 ml). The mixture was degassed via three freeze–pump–thaw cycles. The Schlenk tube was positioned approximately 5 cm away from a 50 W blue LED ($\lambda_{max} = 420$ nm) or 24 W blue LED ($\lambda_{max} = 455$ nm) lamp. After being stirred at −40 °C or 25 °C for the indicated time, the reaction mixture was evaporated to dryness. The residue was purified by flash chromatography on silica gel and eluted with petroleum ether, EtOAc = 5:1, to afford non-racemic product (**37–56**).

Data availability

The data supporting the findings of this study are available from the corresponding author upon request.

Received: 18 March 2019; Accepted: 23 August 2019;
Published online: 07 October 2019

References

1. Labinger, J. A. & Bercaw, J. E. Understanding and exploiting C–H bond activation. *Nature* **417**, 507–514 (2002).
2. Caballero, A. et al. Silver-catalyzed C–C bond formation between methane and ethyl diazoacetate in supercritical CO_2. *Science* **332**, 835–838 (2011).
3. Cook, A. K., Schimler, S. D., Matzger, A. J. & Sanford, M. S. Catalyst-controlled selectivity in the C–H borylation of methane and ethane. *Science* **351**, 1421–1424 (2016).
4. Zhang, Rj. K. et al. Enzymatic assembly of carbon–carbon bonds via iron-catalysed sp^3 C–H functionalization. *Nature* **565**, 67–72 (2018).
5. Prier, C. K., Zhang, R. K., Buller, A. R., Brinkmann-Chen, S. & Arnold, F. H. Enantioselective, intermolecular benzylic C–H amination catalysed by an engineered iron-haem enzyme. *Nat. Chem.* **9**, 629–634 (2017).
6. Cuthbertson, J. D. & MacMillan, D. W. C. The direct arylation of allylic sp^3 C–H bonds via organic and photoredox catalysis. *Nature* **519**, 74–77 (2015).
7. Tran, B. L., Li, B., Driess, M. & Hartwig, J. F. Copper-catalyzed intermolecular amidation and imidation of unactivated alkanes. *J. Am. Chem. Soc.* **136**, 2555–2563 (2014).
8. Mukherjee, S., Maji, B., Tlahuext-Aca, A. & Glorius, F. Visible-light-promoted activation of unactivated C(sp^3)–H bonds and their selective trifluoromethylthiolation. *J. Am. Chem. Soc.* **138**, 16200–16203 (2016).
9. Sharma, A. & Hartwig, J. F. Metal-catalysed azidation of tertiary C–H bonds suitable for late-stage functionalization. *Nature* **517**, 600–604 (2015).
10. Tang, S., Wang, P., Li, H. & Lei, A. Multimetallic catalysed radical oxidative C(sp^3)–H/C(sp)–H cross-coupling between unactivated alkanes and terminal alkynes. *Nat. Commun.* **7**, 11676 (2016).
11. Clark, J. R., Feng, K., Sookezian, A. & White, M. C. Manganese-catalysed benzylic C(sp^3)–H amination for late-stage functionalization. *Nat. Chem.* **10**, 583–591 (2018).
12. Hu, A., Guo, J. J., Pan, H. & Zuo, Z. Selective functionalization of methane, ethane, and higher alkanes by cerium photocatalysis. *Science* **361**, 668–672 (2018).
13. Margrey, K. A., Czaplyski, W. L., Nicewicz, D. A. & Alexanian, E. J. A general strategy for aliphatic C–H functionalization enabled by organic photoredox catalysis. *J. Am. Chem. Soc.* **140**, 4213–4217 (2018).
14. Yi, H. et al. Recent advances in radical C–H activation/radical cross-coupling. *Chem. Rev.* **117**, 9016–9085 (2017).
15. Saint–Denis, T. G., Zhu, R. –Y., Chen, G., Wu, Q. –F. & Yu, J. –Q. Enantioselective C(sp^3)–H bond activation by chiral transition metal catalysts. *Science* **359**, eaao4798 (2018).
16. Rouquet, G. & Chatani, N. Catalytic functionalization of C(sp^2)–H and C(sp^3)–H bonds using bidentate directing groups. *Angew. Chem. Int. Ed.* **52**, 11726–11743 (2013).
17. He, J. et al. Ligand-controlled C(sp^3)–H arylation and olefination in synthesis of unnatural chiral α-amino acids. *Science* **343**, 1216–1220 (2014).
18. Zhang, F. –L., Hong, K., Li, T. –J., Park, H. & Yu, J. –Q. Functionalization of C(sp^3)–H bonds using a transient directing group. *Science* **351**, 252–256 (2016).
19. Choi, G. J., Zhu, Q., Miller, D. C., Gu, C. J. & Knowles, R. R. Catalytic alkylation of remote C–H bonds enabled by proton-coupled electron transfer. *Nature* **539**, 268–271 (2016).
20. Chu, J. C. K. & Rovis, T. Amide-directed photoredox-catalysed C–C bond formation at unactivated sp^3 C–H bonds. *Nature* **539**, 272–275 (2016).
21. Liao, K. et al. Site-selective and stereoselective functionalization of nonactivated tertiary C–H bonds. *Nature* **551**, 609–613 (2017).
22. Liao, K., Negretti, S., Musaev, D. G., Bacsa, J. & Davies, H. M. L. Site-selective and stereoselective functionalization of unactivated C–H bonds. *Nature* **533**, 230–234 (2016).
23. Liao, K. et al. Design of catalysts for site-selective and enantioselective functionalization of non-activated primary C–H bonds. *Nat. Chem.* **10**, 1048–1055 (2018).
24. Fu, J. T., Ren, Z., Bacsa, J., Musaev, D. G. & Davies, H. M. L. Desymmetrization of cyclohexanes by site- and stereoselective C–H functionalization. *Nature* **564**, 395–399 (2018).
25. Mazzarella, D., Crisenza, G. E. M. & Melchiorre, P. Asymmetric photocatalytic C–H functionalization of toluene and derivatives. *J. Am. Chem. Soc.* **140**, 8439–8443 (2018).
26. Zhang, W. et al. Enantioselective cyanation of benzylic C–H bonds via copper catalyzed radical relay. *Science* **353**, 1014–1018 (2016).
27. Li, F. et al. Chiral acid-catalysed enantioselective C–H functionalization of toluene and its derivatives driven by visible light. *Nat. Commun.* **10**, 1774 (2019).
28. Narayanam, J. M. R. & Stephenson, C. R. J. Visible light photoredox catalysis: applications in organic synthesis. *Chem. Soc. Rev.* **40**, 102–113 (2011).
29. Prier, C. K., Rankic, D. A. & MacMillan, D. W. C. Visible light photoredox catalysis with transition metal complexes: applications in organic synthesis. *Chem. Rev.* **113**, 5322–5363 (2013).
30. Chen, J. –R., Hu, X. –Q., Lu, L. –Q. & Xiao, W. –J. Visible light photoredoxcontrolled reactions of N-radicals and radical ions. *Chem. Soc. Rev.* **45**, 2044–2056 (2016).
31. Perry, I. B. et al. Direct arylation of strong aliphatic C–H bonds. *Nature* **560**, 70–75 (2018).
32. Heitz, D. R., Tellis, J. C. & Molander, G. A. Photochemical nickel-catalyzed C–H arylation: synthetic scope and mechanistic investigations. *J. Am. Chem. Soc.* **138**, 12715–12718 (2016).
33. Ackerman, L. K. G., Alvarado, J. I. M. & Doyle, A. G. Direct C–C bond formation from alkanes using Ni-photoredox catalysis. *J. Am. Chem. Soc.* **140**, 14059–14063 (2018).
34. Shen, Y., Gu, Y. & Martin, R. sp^3 C–H arylation and alkylation enabled by the synergy of triplet excited ketones and nickel catalysts. *J. Am. Chem. Soc.* **140**, 12200–12209 (2018).
35. Fan, X. –Z. et al. Eosin Y as a direct hydrogen-atom transfer photocatalyst for the functionalization of C–H bonds. *Angew. Chem. Int. Ed.* **57**, 8514–8518 (2018).
36. Dewanji, A., Krach, P. E. & Rueping, M. The dual role of benzophenone in visible-light/nickel photoredox-catalyzed C–H arylations: hydrogen-atom transfer and energy transfer. *Angew. Chem. Int. Ed.* **58**, 3566–3570 (2019).
37. Xia, J.-B., Zhu, C. & Chen, C. Visible light-promoted metal-free C–H activation: diarylketone-catalyzed selective benzylic mono- and difuorination. *J. Am. Chem. Soc.* **135**, 17494–17500 (2013).
38. Kamijo, S., Kamijo, K., Maruoka, K. & Murafuji, T. Aryl ketone catalyzed radical allylation of C(sp^3)–H bonds under photoirradiation. *Org. Lett.* **18**, 6516–6519 (2016).
39. Li, Y. et al. Copper(II)-catalyzed asymmetric photoredox reactions: enantioselective alkylation of imines driven by visible light. *J. Am. Chem. Soc.* **140**, 15850–15858 (2018).
40. Shen, X. et al. A chiral nickel DBFOX complex as a bifunctional catalyst for visible-light-promoted asymmetric photoredox reactions. *Chem. Sci.* **9**, 4562–4568 (2018).
41. Ma, J. –A. Recent developments in the catalytic asymmetric synthesis of α- and β-amino acids. *Angew. Chem. Int. Ed.* **42**, 4290–4299 (2003).
42. Ravelli, D., Fagnoni, M., Fukuyama, T., Nishikawa, T. & Ryu, I. Site-selective C–H functionalization by decatungstate anion photocatalysis: synergistic control by polar and steric effects expands the reaction scope. *ACS Catal.* **8**, 701–713 (2018).
43. Wang, F. –L. et al. Catalytic asymmetric radical diamination of alkenes. *Chem* **3**, 979–990 (2017).
44. Blanksby, S. J. & Ellison, G. B. Bond dissociation energies of organic molecules. *Acc. Chem. Res.* **36**, 255–263 (2003).
45. Liu, W. et al. Catalyst-controlled selective functionalization of unactivated C–H bonds in the presence of electronically activated C–H bonds. *J. Am. Chem. Soc.* **140**, 12247–12255 (2018).
46. Qin, C. & Davies, H. M. L. Role of sterically demanding chiral dirhodium catalysts in site-selective C–H functionalization of activated primary C–H bonds. *J. Am. Chem. Soc.* **136**, 9792–9796 (2014).
47. Davies, H. M. L. & Hansen, T. Asymmetric intermolecular carbenoid C–H insertions catalyzed by rhodium(II) (*S*)-*N*-(*p*-dodecylphenyl)sulfonylprolinate. *J. Am. Chem. Soc.* **119**, 9075–9076 (1997).
48. Cundari, T. R. et al. Copper-catalyzed C(sp^3)–H amidation: sterically driven primary and secondary C–H site-selectivity. *Angew. Chem. Int. Ed.* **58**, 3421–3425 (2019).
49. Yoon, T. P. Photochemical stereocontrol using tandem photoredox–chiral Lewis acid catalysis. *Acc. Chem. Res.* **49**, 2307–2315 (2016).
50. Bartok, M. Unexpected inversions in asymmetric reactions: reactions with chiral metal complexes, chiral organocatalysts, and heterogeneous chiral catalysts. *Chem. Rev.* **110**, 1663–1705 (2010).
51. Burk, M. J., Allen, J. G. & Kiesman, W. F. Highly regio- and enantioselective catalytic hydrogenation of enamides in conjugated diene systems: synthesis and application of γ,δ-unsaturated amino acids. *J. Am. Chem. Soc.* **120**, 657–663 (1998).

Acknowledgements

We gratefully acknowledge funding from the National Natural Science Foundation of China (grant no. 21572184), the Natural Science Foundation of Fujian Province of China (grant no. 2017J06006) and the Fundamental Research Funds for the Central Universities (grant no. 20720190048).

Author contributions

L.G. and Y.L. conceived and designed the project. Y.L. and M.L. conducted the experiments. Y.L., M.L. and L.G. analysed and interpreted the experimental data. L.G. prepared the manuscript. Y.L. prepared the Supplementary Information.

Competing interests

The authors declare no competing interests.

Additional information

Supplementary information is available for this paper at https://doi.org/10.1038/s41929-019-0357-9.

Correspondence and requests for materials should be addressed to L.G.